HHS Public Access

Author manuscript

Neurobiol Dis. Author manuscript; available in PMC 2016 July 27.

Published in final edited form as:

Neurobiol Dis. 2016 July ; 91: 336–346. doi:10.1016/j.nbd.2016.03.023.

Activation of oligodendroglial Stat3 is required for efficient remyelination

Andrew J. Steelman[a,c,1,2], **Yun Zhou**[a,1], **Hisami Koit**[a], **SunJa Kim**[a,c], **H. Ross Payne**[b], **Q. Richard Lu**[d], and **Jianrong Li**[a,c,*]

[a]Department of Veterinary Integrative Biosciences, College of Veterinary Medicine & Biomedical Sciences, United States

[b]Department of Veterinary Pathobiology, College of Veterinary Medicine & Biomedical Sciences, United States

[c]Institute for Neuroscience, Texas A&M University, College Station, TX 77843, United States

[d]Department of Pediatrics, Brain Tumor Center, Cincinnati Children's Hospital Medical Center, United States

Abstract

Multiple sclerosis is the most prevalent demyelinating disease of the central nervous system (CNS) and is histologically characterized by perivascular demyelination as well as neurodegeneration. While the degree of axonal damage is correlated with clinical disability, it is believed that remyelination can protect axons from degeneration and slow disease progression. Therefore, understanding the intricacies associated with myelination and remyelination may lead to therapeutics that can enhance the remyelination process and slow axon degeneration and loss of function. Ciliary neurotrophic factor (CNTF) family cytokines such as leukemia inhibitory factor (LIF) and interleukin11(IL-11) are known to promote oligodendrocyte maturation and remyelination in experimental models of demyelination. Because CNTF family member binding to the gp 130 receptor results in activation of the JAK2/Stat3 pathway we investigated the necessity of oligodendroglial Stat3 in transducing the signal required for myelination and remyelination. We found that Stat3 activation in the CNS coincides with myelination during development. Stimulation of oligodendrocyte precursor cells (OPCs) with CNTF or LIF promoted OPC survival and final differentiation, which was completely abolished by pharmacologic blockade of Stat3 activation with JAK2 inhibitor. Similarly, genetic ablation of Stat3 in oligodendrocyte lineage cells prevented CNTF-induced OPC differentiation in culture. In vivo, while oligodendroglial Stat3 signaling appears to be dispensable for developmental CNS myelination, it is required for oligodendrocyte regeneration and efficient remyelination after toxin-induced focal demyelination in the adult brain. Our data suggest a critical function for oligodendroglial Stat3 signaling in myelin repair.

*Corresponding author at: Department of Veterinary Integrative Biosciences and, Institute for Neuroscience, Texas A&M University, Mail Stop 4458, College Station, TX, 77843, United States. jrli@cvm.tamu.edu (J. Li).

[1]Contributed equally to this study.

[2]Present address: Department of Animal Sciences, University of Illinois at Urbana-Champaign.

Keywords

Oligodendrocyte maturation; Stat3 signaling; Myelination; Remyelination; CNTF

1. Introduction

Multiple sclerosis (MS) is a degenerative disease of the central nervous system that is characterized by primary demyelination, leukocyte infiltration, axon transection and neurodegeneration. While the cause of MS remains unknown, many lines of evidence have demonstrated that this disease is perpetuated by aberrant inflammation of the brain and spinal cord. Remyelination can occur in some MS patients but is lost overtime (Franklin and ffrench-Constant, 2008). The progressive worsening of neurological function in MS patients is likely attributable to a complex interplay between inflammatory myelin destruction and reparation failure (Franklin and ffrench-Constant, 2008). To this end, it has been suggested that repeated inflammatory attacks superimposed on persistently demyelinated axons facilitates neurodegeneration, cerebral atrophy and loss of function (Compston and Coles, 2008). While current immunomodulatory therapeutics are able to effectively reduce relapses, they do not prevent the progressive loss of neurological function in MS patients, suggesting that reparation failure may predispose axons to secondary degeneration (Franklin et al., 2012; Irvine and Blakemore, 2008; Nave, 2010). As such, promoting the capacity of remyelination may not only improve functional recovery but also protect axons from further damage (Irvine and Blakemore, 2008). Understanding the mechanisms that promote remyelination is therefore essential for the development of truly effective therapeutics which may slow the unrelenting loss of function in MS patients.

Remyelination is a spontaneous repair process that occurs naturally following demyelination (Blakemore, 1972, 1973). However, in order for efficient remyelination to occur a complex series of events must transpire, which includes oligodendrocyte precursor cell (OPC) recruitment to the lesion site, proliferation, differentiation and finally ensheathing of denuded axons (Franklin and ffrench-Constant, 2008). Inhibition of this process at any of the above steps results in remyelination failure and increased susceptibility to neuronal degeneration (Franklin, 2002). Therefore, identification of specific factors and/or signaling pathways that enable CNS myelin repair is a prerequisite for the development of reparative therapeutics in demyelinating diseases.

Activation of the shared glycoprotein (gp)130 receptor by the ciliary neurotrophic factor (CNTF) family cytokines such as CNTF, leukemia inhibitory factor (LIF), cardiotrophin-1, oncostatin M, and IL-11 has been shown to promote oligodendrocyte (OL) survival (Barres et al., 1993; Butzkueven et al., 2002; Kerr and Patterson, 2005; Louis et al., 1993; Zhang et al., 2006), trafficking (Vernerey et al., 2013), maturation (Stankoff et al., 2002), myelination (Ishibashi et al., 2006; Zhang et al., 2011), and remyelination (Marriott et al., 2008; Zhang et al., 2006). Additionally, CNTF- and LIF-mediated gp130 receptor activation appears to be neuroprotective as loss of endogenous CNTF, antagonism of LIF, and disruption of gp130/LIFR-β signaling all result in increased disease severity in MOG-induced experimental autoimmune encephalomyelitis (EAE), an animal model of MS (Butzkueven et al., 2002;

Linker et al., 2002; Lu et al., 2009). Moreover, *Cntf*$^{-/-}$ (Barres et al., 1996) and *Lif*$^{-/-}$ (Ishibashi et al., 2009) mice exhibit delayed myelination of the optic nerve during development. However, the intracellular signaling process that drives these events has not been well characterized.

Stat3 is a major signaling and transcription factor downstream of gp130 receptor activation. Genetic deletion of SOCS3, an endogenous negative regulator of Stat3 signaling, specifically in mature oligodendrocytes, protects against cuprizone mediated demyelination (Emery et al., 2006). However, the direct contribution of oligodendroglial Stat3 signaling to developmental myelination and remyelination processes remains elusive. Herein, utilizing oligodendrocyte lineage cell-specific Stat3 conditional mice, we report that Stat3 activation mediates the effect of CNTF on oligodendroglial survival and differentiation in vitro and that activation of Stat3 signaling in oligodendrocyte lineage cells is necessary for efficient myelin repair after focal toxin-induced demyelination in the adult CNS.

2. Materials and methods

2.1. Animals

Sprague Dawley rats were obtained from Harlan Laboratories. Transgenic *Plp1CreER*^{T} mice encoding a *Plp1* promoter driven Cre recombinase fused to a mutant estrogen receptor that is activated by tamoxifen have been described previously (Doerflinger et al., 2003) and were obtained from the Jackson Laboratory (Bar Harbor, MA). *Olig1Cre* heterozygous mice expressing Cre recombinase under the endogenous *Olig1* promoter with the *neo* selection cassette removed were described previously (Xin et al., 2005). *Stat3*$^{fl/fl}$ mice containing LoxP sites flanking exons 21&22, which encode the tyrosine residue (Y705) essential for Stat3 transcriptional activity, have been previously described (Takeda et al., 1998) and were backcrossed eight generations to a C57BL/6 background prior to use. Conditional mutant mice were generated by cross-breeding *Stat3*$^{fl/fl}$ with *Plp1CreER*^{T} or *Olig1Cre* mice. C57BL/6, B6.129×1-Gt(ROSA)26Sortm1(EYFP)Cos/J (Rosa26) and B6.129S6-Gt(ROSA)26Sortm14(CAG-tdTomato)Hze/J (Ai14) reporter mice were obtained from the Jackson Laboratory (Bar Harbor, ME). All animals were housed under constant 12-h light/dark cycles in covered cages and fed with a standard rodent diet ad libitum. The experimental procedures described herein were approved by the Institutional Animal Care and Use Committee and were performed in accordance with guidelines of the National Institutes of Health.

2.2. Isolation of primary cultures

Mixed glial cultures and oligodendrocyte precursor cells (OPCs) were isolated with the differential attachment method as described previously (Chen et al., 2007; Kim et al., 2011; Li et al., 2008). In brief, the brains of P1–2 rat or mouse pups were isolated and placed in ice cold HBSS, followed by meninges removal under a dissection microscope. The brain tissues were disassociated with Trypsin (0.01%) and DNase (10 μg/ml) at 37 °C for 15 min. After washing with ice cold DMEM the cells were passed through a 70 μm filter and plated onto poly-d-lysine-coated coverslips or T-flasks and grown to confluence (days in vitro (DIV) 7–10) in a humidified incubator at 37 °C and 5% CO_2. For OPC isolation, the T-flasks were

shaken at 37°C for 1 hat200 rpm to remove microglia followed by overnight shaking. Cell suspension collected from the flasks was plated twice onto petri dishes to further remove microglia and astrocytes. The highly enriched OPCs were then collected by centrifugation, passing through sterile screening pouch (20 μm), and cultured in a serum-free growth medium, Basal Defined Medium(BDM) (DMEM containing 0.1% bovine serum albumin, 50 μg/ml human apotransferrin, 50 μg/ml insulin, 30 nM sodium selenite, 10 nM D-biotin, and 10 nM hydrocortisone) supplemented with recombinant human PDGF-aa (10 ng/ml, Peprotech) and bFGF (10 ng/ml, Peprotech). The purity of enriched oligodendroglial cultures was consistently greater than 95% (Kim et al., 2011; Li et al., 2008; Steelman et al., 2013). Other cytokines used were recombinant rat CNTF (10 ng/ml, Peprotech), human LIF (10 ng/ml, Alomone Labs), human IL-6 (100 ng/ml, Cell Signaling Tech) and rat IL-6 (10 ng/ml, eBioscience). For OPC differentiation studies BDM medium devoid of PDGF-aa and bFGF was used.

2.3. Western blot

Antibodies against P-Stat3 (S727, 1:1000), P-Stat3 (Y705, 1:1000), total Stat3 (1:1000), Bcl-2 (1:1000), caspase-3 (1:1000), CNPase (1:1000) and MBP (1:1000) were from Cell Signaling Technology (Danvers, MA). Antibodies for Cre (1:2000) and β-actin (1:10000) were purchased from Sigma. Western blotting analysis was carried out as described (Kim et al., 2012; Steelman et al., 2013). Briefly, cells were lysed on ice in lysis buffer (1% Triton X-100, 20 mM Tris, pH 7.5, 150 mM NaCl, 1 mM EDTA, 1 mM EGTA, 10 mM $Na_2P_2O_7$, 10 mM NaF, 1 mM Na_3VO_4, 1 mM PMSF) containing proteinase inhibitor mixture I (Roche Applied Science), sonicated, and then centrifuged to remove cellular debris. Proteins were separated on polyacrylamide gels by SDS-PAGE, transferred to PVDF membranes, blocked with TBST (50 mM Tris-HCl, pH 7.4, 150 mM NaCl, 0.1% Tween 20) containing 5% nonfat milk or 1% bovine serum albumin (BSA) and probed with the primary antibodies overnight at 4 °C. The membranes were incubated with appropriate HRP-conjugated secondary antibodies for 1 h at RT and visualized by chemiluminescence using the West Pico ECL reagent (Thermo Scientific, Rockford, IL). Western blot images were acquired with a Bio-Rad Chemidoc XRS gel documentation system and quantified with Quantity One software.

2.4. Viral infection of OPCs

Since primary oligodendrocytes are difficult to transfect, retroviral vectors containing constitutively active Stat3 (Stat3-CA) were constructed (Xie et al., 2004). Substitution of two cysteine residues within the C-terminal loop of the SH2 domain of Stat3 causes spontaneous dimerization and activation of transcription (Bromberg et al., 1999). The Stat3-CA vector was amplified by PCR and subcloned into the retroviral vector MIEG3 containing an eGFP co-expression cassette to facilitate identification of infected cells (a gift from Dr. Qishen Pang, Cincinnati Children's Hospital Medical Center) (Williams et al., 2000). The MIEG3 and MIEG-Stat3-CA plasmids were used to produce retroviral supernatant from transfected Phoenix-Ampho packaging cells (American Type Culture Collection, Manassas, VA) as detailed previously (Williams et al., 2000). Rat OPCs (DIV1) were incubated with virus-containing supernatant for 24 h, followed by medium removal and addition of fresh viral supernatant for an additional 24 h. After the final removal of virus-containing medium,

OPCs were recovered in growth medium for one day, switched to BDM for 2 days, and then the morphology of $eGFP^+$ cells was analyzed by fluorescence microscopy. In some studies the effect of Stat3 signaling in mixed glial cultures was determined following transfection of *Stat3*$^{fl/fl}$ glia with an adenoviral eGFP vector (control) or adenoviral Cre-eGFP (University of Iowa Gene Transfer Vector Core) as described previously (Li et al., 2008). After the removal of recombinant adenovirus, cells were allowed to recover for one day and then cultured in BDM in the presence or absence of CNTF for additional 2 days, and analyzed by immunocytochemistry.

2.5. Immunocytochemistry

Following treatment, cells were fixed with 4% paraformaldehyde (PFA) in PBS for 10 min, washed and blocked with TBS (50 mM Tris-HCl, pH 7.4, 150 mM NaCl) containing 5% goat serum for A2B5 and O4 immunostaining (Li et al., 2008). After overnight incubation with mouse anti-A2B5 or O4 antibodies (1:200) and washing, the cells were incubated with fluorophore conjugated anti-mouse IgM (Invitrogen, Carlsbad, CA; 1:1000) and post-fixed. The cells were then permeabilized with 0.1% Triton-X 100 in TBS (TBST) containing 5% goat serum for 1 h, and then incubated with anti-P-Stat3 (Y705, 1:100, Cell Signaling), anti-NG2 (1:200, rabbit IgG, Chemicon), anti-Olig2 (1:500, rabbit IgG, Millipore), anti-PLP (1:500; AA3), anti-MBP (1:500, rabbit IgG; Millipore) or anti-GFP (1:100; Invitrogen, Carlsbad, CA) overnight at 4 °C. After washing with TBST, appropriate fluorophore conjugated secondary antibodies were added and incubated for 1 h at room temperature. The cells were counter stained with Hoechst 33258 (bis-benzimide, Invitrogen, Carlsbad, CA), and images were captured using an Olympus DP70 digital camera mounted on an Olympus IX71 microscope.

2.6. Animal model of chemically induced focal demyelination and remyelination

Mice (10–12 weeks) were anesthetized by i.p. injection of ketamine (100 mg/kg) and xylazine (10 mg/kg) in a total volume of 0.1 ml sterile phosphate buffered saline (PBS; pH 7.4). Upon reaching a surgical plane of anesthesia the mice were secured in a stereotaxic frame (Kopf; Tujunga, CA) and a focal area of demyelination in the rostral corpus callosum was induced by injection of 2 μl L-α-lyso-lecithin (1%; Calbiochem) at a rate of 0.2 μl/min using a Hamilton syringe fitted with a 32G needle into the following coordinates with respect to Bregma: AP = 1.2 mm, LV = 1.0 mm, DV = −2.0 mm. In this model, focal demyelination occurs acutely 1–3 days post lesion (dpl) followed by regenerative responses including OPC migration and proliferation into the lesion (3–7 dpl), differentiation into myelin-producing OLs (7–14 dpl) and active remyelination (14–21 dpl) (Etxeberria et al., 2010; Huang et al., 2011). The extent of myelin repair was compared between control and Stat3 mutant mice at 7, 14 and 21 days post injection. At specified time-point, mice were anesthetized, transcardially perfused with 4% PFA in PBS. After removal, the brains were kept in fresh fixative overnight at 4 °C, transferred to 30% sucrose (w/v) in PBS and kept at 4 °C until sunk. The brains were frozen in optimal cutting temperature (OCT) solution and serial coronal sections (10 μm) were collected through the entire lesioned area using a cryostat (Leica CM 1950; Buffalo Grove, IL). The analysis of lesion length included rostral-caudal measurement of all slide sections containing a lesion. Analyses of cell counts

included only those slide sections with the lesion initiating from the needle tract and spanning at least 500 μm rostral-caudally (corresponding to at least 5 sections per mouse).

2.7. Histochemistry, immunohistochemistry and lesion analysis

Myelin was stained with Oil Red O as described previously (Kim et al., 2012; Steelman et al., 2013). Stat3-expressing cells during the CNS development was evaluated with rabbit and mouse monoclonal antibodies (Cell Signaling Tech). Immunofluorescence microscopy was used to assess differences between genotypes using antibodies against PLP, MBP, Olig2, and CC1 as described (Steelman et al., 2012). For remyelination studies, representative coronally sectioned slides encompassing the entire lesion were stained with Oil Red O. Lesion length was estimated by determining the difference in the anatomic location at the initiation and the end of the lesion in Oil Red O stained sections using the mouse brain atlas (Franklin and Paxinos, 2008). Serial sections were stained for PLP, Olig2, CC1, NG2, Iba-1 and GFAP. Briefly, brain sections were incubated at 37 °C for 30 min then rehydrated with PBS for 10 min. The sections were blocked and permeabilized with 0.3% Triton-X 100 in PBS containing 5% goat serum for 1 h at room temperature, followed by overnight incubation at 4 °C with primary antibodies, rat anti-PLP (AA3; 1:500), rabbit anti-Olig2 (1:200), mouse anti-CC1 (1:200), rabbit NG2 (1:200), rabbit anti-Iba-1 (1:1000) and chicken anti-GFAP (1:100) in PBS containing 0.1% Triton-X 100. After washing, the sections were incubated with appropriate fluorophore conjugated goat secondary antibodies (1:1000; Invitrogen). Nuclei were stained with bis-benzimide Hoechst 33258. The extent of demyelination was analyzed using PLP and Hoechst 33258 stained sections with ImageJ (Schneider et al., 2012). Specifically, 4× fluorescence images containing the lesions were captured at a constant exposure time, transformed into binary images and then stacked using ImageJ. The lesion area in each image was outlined by tracing the hypercellular area in the corpus callosum based on Hoechst 33258 staining and the percentage of the area that was PLP negative was calculated. The numbers of mature ($CC1^+$) and total $Olig2^+$ OL lineage cells within the lesions were determined by stacking 10× images of Hoechst 33258, CC1 and Olig2 stained sections and counting the number of positive cells. For each measurement at least five to six sections spanning 500–600 μm were analyzed per mouse and averages of each mouse were used to compare each group.

2.8. Transmission electron microscopy

Mice at specified ages were fixed by transcardial perfusion with 2.5% glutaraldehyde and 4% paraformaldehyde in PBS (pH 7.3). After dissection, tissues were post-fixed in 1% osmium tetroxide in 0.1 M Na cacodylate buffer, dehydrated in an ascending alcohol series and embedded in Embed812/Araldite epoxy resin (Electron Microscopy Sciences, Hatfield, PA). Semi-thin sections, 400 nm-thick, were stained with the solution of 0.5% methylene blue and 0.5% Azure II. Ultra-thin sections (60 to 90 nm thick) were cut with a Leica EM UC6 ultramicrotome, post-stained in 2% aqueous uranyl acetate followed by lead citrate and examined with an FEI Morgagni 268 transmission electron microscope at an accelerating voltage of 80 kV. Digital images were acquired with a MegaViewIII camera operated with iTEM software (Olympus Soft Imaging Systems, Germany).

2.9. Statistical analysis

The data were analyzed using two-tailed Student's t tests for comparisons between two groups as well as multiple level analysis of variance followed by Bonferroni's post hoc test when comparing more than two groups. All analysis was performed using GraphPad Prism (GraphPad Software, San Diego, CA). Groups were considered to be different when $p \leq 0.05$.

3. Results

3.1. Oligodendrocyte lineage cells express Stat3 in vitro and in vivo

To investigate the potential role of Stat3 in CNS myelinogenesis, we first examined the temporal expression pattern of Stat3 during normal brain development. In rodents, CNS myelination occurs primarily during the second and third postnatal weeks, and is nearly complete by the fourth postnatal week. Total Stat3 was detectable as early as embryonic day 16 (E16) and remained relatively constant at all time-points examined in both the cerebrum (Fig. 1A; left) and cerebellum (Fig. 1A; right). In contrast, activation of Stat3 (P-Tyr705, unless stated otherwise) became evident at P13 and remained activated at P30 (Fig. 1A). Overall, Stat3 activation during postnatal brain development correlated well with myelinogenesis as determined by MBP expression (Fig. 1A) and also coincided with astrogliogenesis, which has been previously shown requires Stat3 signaling (Bonni et al., 1997; He et al., 2005). In addition, the temporal activation of Stat3 in the developing brain also correlated with neuronal maturation during the postnatal development (Dziennis and Alkayed, 2008). Immunohistochemical analysis at P14 revealed total Stat3 expression in subsets of cells that morphologically resembled neurons, endothelial cells and astrocytes (Fig. 1B and not shown). However, a substantial number of $Stat3^+$ cells colocalized with $CC1^+$ cells in the cortex, cingulate gyrus (Fig. 1B) and corpus callosum (Fig. 1C, D), raising the question whether Stat3 signaling could be involved in oligodendrocyte differentiation and myelination.

3.2. CNTF activates Stat3 and promotes OL lineage cell survival and differentiation

It has been demonstrated previously that OPCs express JAK1/2 but have relatively low levels of Tyk2 and that stimulation of these cells with CNTF results in Stat3 activation (Dell'Albani et al., 1998) and maturation (Stankoff et al., 2002). To understand the function of Stat3 in myelination process, we questioned if CNTF driven Stat3 activation was restricted to specific developmental stages of oligodendrocyte lineage cells. Treatment of purified OL cultures with CNTF induced Stat3 nuclear translocation in a manner that was not restricted to a specific OL developmental stage (Fig. 2A, B). CNTF treatment activated P-Stat3 and increased the expression of CNPase and MBP as well as antiapoptotic protein Bcl-2 (Fig. 2C). Likewise, CNTF significantly enhanced OL viability (Fig. 2D) and decreased the percentage of OLs undergoing apoptotic cell death in culture (Fig. 2E). Together these data demonstrate a strong correlation between CNTF-induced Stat3 activation and increased OL survival and differentiation.

3.3. Pharmacological blockade of Stat3 activation prevents CNTF-induced OL survival and differentiation

We next examined whether pharmacological blockade of Stat3 activation abolishes the effect of CNTF on OL survival and maturation. Treatment of OL cultures with the JAK2 inhibitor AG490 diminished CNTF-induced Stat3 activation, Bcl2 expression and OL differentiation (Fig. 3A) in agreement with a previous study (Stankoff et al., 2002). Immunocytochemical analysis further revealed a decrease in OL maturation and survival of cultures treated with AG490 (Fig. 3B–D). Of note, spontaneous differentiation of OPCs after withdrawal of mitogens PDGF-AA and FGF-2 was also inhibited by the JAK2 inhibitor (Fig. 3A, C). Two other members of the CNTF family, LIF, which promotes OL differentiation and survival, and IL-6, which has minimum effect on OL maturation (Stankoff et al., 2002), were then examined for their capability to activate Stat3 signaling. Phosphorylation of Stat3 at both tyrosine 705 and serine 727 residues were significantly elevated in oligodendroglia following treatment with LIF but not with IL-6 (Fig. 3E). Interestingly, LIF but not IL-6 promoted OL differentiation (Fig. 3E). Consistent with the idea that the Stat3 pathway promotes OL maturation, AG490 prevented LIF-induced Stat3 phosphorylation and OL differentiation as determined by MBP expression (Fig. 3E). Primary OLs are known to undergo spontaneous apoptosis in culture over time after mitogen withdrawal. Activation of caspase-3 was evident in these cultures and was exacerbated following AG490 treatment, which also markedly downregulated Bcl2 (Fig. 3E). It should be pointed out that while both CNTF and LIF enhanced OPC maturation and survival, IL-6 did not significantly affect this process (Fig. 3A, E, and data not shown), likely due to differences in the components of the receptor complex formed upon the cytokine stimulation (Stankoff et al., 2002). Collectively, these data suggest that LIF and CNTF mediated Stat3 activation promotes OL maturation and survival.

3.4. Stat3 is required to promote OPC differentiation in vitro

Next, we questioned if persistent activation of Stat3 was sufficient to drive OPC differentiation. We ectopically expressed constitutively activated Stat3 (Stat3-CA) (Bromberg et al., 1999; Xie et al., 2004) in OPC cultures and analyzed the morphology of transfected GFP^+ OPCs. While the majority of OPCs transfected with the control viral vector containing GFP were bipolar, the OPCs transfected with Stat3-CA had a significantly higher percentage of cells with tertiary processes (Fig. 4A), indicating that activated Stat3 facilitates OPC branching. In congruent with this observation, further immunocytochemistry analysis of GFP^+ cells showed that in comparison to control vector, Stat3-CA transfection resulted in a lower percentage of $A2B5^+$ progenitors with category I morphology (26% versus 44% in controls) and higher percentage of $CNPase^+$ OLs in category III (43% versus 16% in controls).

To further determine if Stat3 activation is required for the pro-differentiation effect of CNTF, we inactivated Stat3 pathways through Cre recombinase-mediated excision of floxed Stat3. OPCs derived from $Stat3^{fl/fl}$ mice were transfected with recombinant adenovirus containing either GFP (AdGFP) or Cre-GFP (AdCre-GFP) (Fig. 4B). Treatment of AdGFP-transduced OPCs with CNTF increased the number of PLP^+ OLs in the culture (Fig. 4C), however, this

effect was significantly suppressed in AdCre-GFP transduced OPCs (Fig. 4C), indicating that Stat3 is, at least in part, responsible for the pro-differentiation effect of CNTF.

Although highly enriched OPC cultures were used in the above experiments, the possibility of other contaminating cells such as astrocytes that may indirectly affect OPC maturation and survival in a Stat3-dependent manner could not be excluded since viral transfection and pharmacological inhibitors do not discriminate different cell types and can target all cells. To determine definitively whether Stat3 signaling is essential to CNTF-induced OPC maturation and survival in vitro, and most importantly its function in vivo, we then employed genetic approaches to selectively ablate *Stat3* in OL lineage cells. Conditional Stat3 mutant mice in which *Stat3* is specifically targeted in OL lineage cells were generated by crossing *Stat3*$^{fl/fl}$ mice to *Olig1Cre* mice (Lu et al., 2002; Xin et al., 2005). Mixed glial cultures were derived from *Stat3*$^{fl/fl}$ or *Olig1Cre:Stat3*$^{fl/fl}$ neonatal pups and cultured in growth medium for 1 week prior to switching to BDM containing either vehicle or CNTF. In agreement with our above results, CNTF significantly increased the percentage of mature MBP^{+}O4^{+} OLs in *Stat3*$^{fl/fl}$ cultures in a time-dependent fashion (Fig. 4D). However, this pro-differentiation effect of CNTF was nearly completely abrogated in *Olig1Cre:Stat3*$^{fl/fl}$ cultures where Stat3 signaling was specifically inactivated in OL lineage cells (Fig. 4D). Similar effects were also observed for LIF (not shown). Together, these results suggest that activation of oligodendroglial Stat3 signaling pathways is required for CNTF-induced oligodendrocyte differentiation and/or survival in vitro.

3.5. Oligodendrocyte Stat3 is dispensable for developmental myelinogenesis

To investigate whether loss of Stat3 signaling in oligodendrocyte lineage cells affects CNS myelination during development, we initially compared myelin formation between *Stat3*$^{fl/fl}$ mice and *Plp1CreER-*^{T}*:Stat3*$^{fl/fl}$ mice that harbor a tamoxifen-inducible, *Plp1*-driven Cre recombination system (Doerflinger et al., 2003). Early experiments with *Plp1CreER*^{T} reporter mice showed that repeated tamoxifen injection (i.p.) into the nursing mother caused a substantial number of PLP^{+} cells undergoing Cre-mediated recombination in the offspring (Supplementary Fig. 1). However, under these experimental conditions, we were unable to detect any differences in the extent of myelination between *Stat3*$^{fl/fl}$ and *Plp1CreER*^{T}*:Stat3*$^{fl/fl}$ mice in either the spinal cord or brain at P14 (Supplementary Fig. 2A–C). Because *Lif*$^{-/-}$ mice display transient delay in myelination of the optic nerve at P10 (Ishibashi et al., 2009), we then examined if *Stat3* inactivation affects optic nerve myelination and found no differences between the control and mutant mice by immunohistochemical or ultrastructural analysis (Supplementary Fig. 2D–E).

Since *Plp1* is mostly active in differentiating OLs, it is possible that the absence of an effect of Stat3 on myelination is due to the fact that *Stat3* signaling in OPCs rather than in differentiated OLs is important for myelination. Therefore, we generated *Olig1Cre:Stat3*$^{fl/fl}$ mice where *Stat3* can be targeted specifically and efficiently in OL lineage cells including OPCs during development (Lu et al., 2002; Xin et al., 2005). Consistent with previous reports, Cre-mediated recombination, as demonstrated with the *Olig1Cre:Rosa26-tdTomato* reporter mice, was evident in cells that morphologically resembled OLs and co-localized with Olig2 immunostaining (Supplementary Fig. 3A). However, again we did not find

differences in CNS myelination between *Stat3*$^{fl/fl}$ and *Olig1Cre:Stat3*$^{fl/fl}$ mice (Supplementary Fig. 3). Moreover, ultrastructural analysis of spinal cord sections of miceat12 months of age showed normal myelin structure and no apparent deficit in myelin maintenance in *Olig1Cre:Stat3*$^{fl/fl}$ mice (Supplementary Fig. 4). Consistent with these results, *Olig1Cre:Stat3*$^{fl/fl}$ mice were phenotypically indistinguishable from *Stat3*$^{fl/fl}$ mice. Collectively, these data strongly indicate that Stat3 signaling in oligodendrocyte lineage cells is dispensable for CNS myelination during normal development.

3.6. Stat3 signaling in oligodendrocyte lineage cells promotes remyelination following focal demyelination

To investigate whether Stat3 plays a role in remyelination after injury, we employed a well-established lysolecithin (LPC)-induced demyelination/remyelination model. In this model, chemically induced focal demyelination is followed by a robust, spontaneous regenerative process, comprising OPC migration and proliferation into the lesion (3– 7 days post lesion (dpl)), differentiation into myelin-producing OLs (7–14 dpl) and active remyelination (14–21 dpl) (Etxeberria et al., 2010; Huang et al., 2011; Wegener et al., 2015). CNTF expression has been previously shown to be upregulated during the peak of demyelination (Vernerey et al., 2013) as well as during the remyelination phase ((Huang et al., 2011). IL-11, an inducer of gp130-mediated Stat3 activation, has also been shown to contribute to myelin regeneration (Zhang et al., 2011). We induced demyelination by stereotaxic injection of LPC into the rostral region of the corpus callosum of adult *Stat3*$^{fl/fl}$ and *Olig1Cre:Stat3*$^{fl/fl}$ mice (Fig. 5A) and examined the extent of myelin repair process 7, 14 and 21 days later. Demyelination and myelin debris were evident at 7 dpl in both control and Stat3 mutant mice when visualized with oil red O histological staining (Fig. 5A) and is associated with robust activation of microglia/macrophages (Supplementary Fig. 5). Myelin debris expanding cross the callosal midline was observed in mutant mice at 7 dpl, suggesting exacerbated demyelination. Similarly, although the lesion size, as determined by the area of hypercellularity, was not statistically different between genotypes, demyelination as quantified by PLP negative area within the lesion was greater in *Olig1Cre:Stat3*$^{fl/fl}$ mutant mice compared to littermate *Stat3*$^{fl/fl}$ controls at both 7 dpl and 14 dpl (Fig. 5B & C). Interestingly, the total number of Olig2^{+} OL lineage cells in the lesion was comparable between the two genotypes (Fig. 5D, E), however, the percentage of CC1^{+} differentiated OLs was significantly lower in lesions of Stat3 mutant mice with respect to control mice (Fig. 5D, F). This marked suppression of CC1^{+} OLs formation in the lesion of *Olig1Cre:Stat3*$^{fl/fl}$ mice was not due to a shortage of OPCs as *Olig1Cre:Stat3*$^{fl/fl}$ mice had similar number of NG2^{+} progenitor cells in the lesion compared to the control mice (Fig. 5G). These data suggest that Stat3 signaling promotes OPC differentiation in demyelinated lesions.

To determine the effect of oligodendroglial Stat3 inactivation on remyelination, we analyzed transmission electron micrographs of the lesion area at 14 and 21 days post injection. Ultrastructural analysis confirmed that *Olig1Cre:Stat3*$^{fl/fl}$ mice had drastically decreased number of myelinated axons in the lesion in comparison with littermate controls at 14 dpl (Fig. 5H, I). Consistently, while thinly remyelinated axons were frequently observed in the control mice, they were rarely detected in *Olig1Cre:Stat3*$^{fl/fl}$ mice where the majority of

axons remained demyelinated (Fig. 5I). Quantification of *g*-ratios (ratio of axon diameter over fiber diameter) of (re)myelinated axons in the lesion further confirmed less extent of remyelination of callosal axons in the mutant mice (Fig. 5J, K). To determine if the lack of remyelination in *Olig1Cre:Stat3*$^{fl/fl}$ mice at 14 dpl persists over time, we analyzed remyelination at 21 dpl (Fig. 6). We found that the density of CC1^{+} differentiated OLs increased gradually from 7 to 21 days post-injection in both genotypes (Fig. 6B), but the mutant mice had significantly less differentiated OLs in the lesion and the proportion of unmyelinated axons at 21 dpl remained significantly higher in the mutant mice than littermate controls (Fig. 6C, D, E). In agreement, *g*-ratios of remyelinated axons were markedly higher in the *Stat3* mutantmice than those of control mice, which correspond to thinner myelin sheaths (Fig. 6 E, F). Together, these data demonstrate that loss of Stat3 signaling in OL lineage cells impedes OL differentiation and myelin repair processes following LPC-induced focal demyelination in vivo (Supplementary Fig. 6).

4. Discussion

In this study we investigated the role of Stat3 in oligodendrocyte maturation during development and remyelination. We found that although Stat3 activation overtly correlates with myelination during postnatal CNS development, *Plp1 or Olig1* promoter-driven conditional deletion of Stat3 is not sufficient to alter developmental myelination kinetics and myelin ultrastructure. In contrast, we found that Stat3 activation following CNTF or LIF stimulation of oligodendrocyte precursor cells is required to promote maturation *in vitro*. Most importantly, we provided *in vivo* evidence that oligodendrocyte-lineage specific Stat3 signaling is needed for efficient regenerative processes and remyelination following toxicant-induced focal demyelination in the adult brain. To our knowledge this report represents the first that employed lineage specific gene targeting approach that demonstrated a key role for oligodendrocyte Stat3 signaling in myelin repair *in vivo.*

Our findings that endogenous Stat3 signaling in oligodendrocyte lineage cells is not essential to normal developmental myelination is in line with previous studies that showed only transiently delayed oligodendrocyte generation and myelination in the optic nerve of *Cntf*$^{-/-}$ (Barres et al., 1996) and *Lif*$^{-/-}$ (Ishibashi et al., 2009) mice. We found that Stat3 activation in the rodent brain in general correlates with the onset of MBP expression and myelination. However, when we used the *Plp1* promoter driven inducible Cre line to genetically ablate Stat3, we were unable to detect alterations in myelination kinetics in the spinal cord, brain, or optic nerve. Similar results were obtained with *Olig1Cre* mediated targeting of Stat3 in oligodendrocyte lineage cells, insofar as we observed no apparent differences in myelination during normal development. Interestingly, genetic null mutation of *Plp1* or oligodendrocyte specific mutation of *Cnp1* or *Pex5* also seems to have limited effects on myelination, but results in altered neural trophic support and progressive neurodegeneration (Nave, 2010). As such, we tested whether conditionally deletion of Stat3 in oligodendrocyte lineage cells results in minor alterations in myelin ultrastructure that manifests itself as axonal degeneration and loss of function much later in life, similar to that observed in *Plp1* null and *Cnp1* mutant mice. However, we did not observe progressive neurodegeneration in *Olig1:Stat3* mutant mice at one year of age. Thus, genetic targeting of Stat3 signaling specifically in OL lineage cells did not compromise developmental myelinogenesis.

Congruent with our findings, a recent study also showed that although NG2-driven conditional ablation of gp130 in OL lineage cells prevented the proliferative effect of exogenously delivered LIF on OPCs *in vivo*, it did not affect OPC cycling in the absence of exogenous LIF nor appeared to result in hypomyelination during development, suggesting that selective loss of gp130 signaling in OL lineage cells does not significantly affect developmental myelination (Deverman and Patterson, 2012). Together, these data strongly suggest that Stat3 signaling in oligodendrocytes is dispensable for myelination during normal postnatal development.

The effects of gp130 receptor ligands on oligodendrocytes have been extensively studied and collectively reveal a potent regenerative role for these cytokines following demyelination (Albrecht et al., 2007; Deverman and Patterson, 2012; Marriott et al., 2008; Modi et al., 2013; Stankoff et al., 2002; Vernerey et al., 2013). For instance, LPC-induced demyelination has recently been shown to promote the upregulation of CNTF as early as four days post injection resulting in enhanced OPC trafficking and proliferation (Vernerey et al., 2013). LIF-deficient mice exhibit more OL loss and demyelination in the cuprizone model (Emery et al., 2006). Cerebral delivery of LIF-encoding but not control adenovirus increases OPC trafficking and promotes remyelination following cuprizone-induced demyelination (Deverman and Patterson, 2012). Moreover, secretion of LIF by intracerebrally transplanted iPSCs promotes OPC proliferation, maturation, and myelination in the EAE model of MS (Laterza et al., 2013). Mice in which *Il-11* is inactivated have delayed remyelination following LPC-induced demyelination and *in vitro* knockdown of Stat3 via siRNA prevents IL-11 induced OPC maturation (Zhang et al., 2011). Our results are in line with these previous studies, and show that selective inactivating *Stat3* within the OL lineage cells impedes OL differentiation and remyelination after acute demyelinating insult *in vivo.* Why endogenous oligodendroglial Stat3 signaling is dispensable for myelination under physiological conditions but is required for the efficient myelin regenerative process after foal demyelinating injury is not clear at present. However, cellular responses after focal demyelinating insult and their extracellular milieu in the adult brain are drastically different from that of development. Marked up-regulation of cytokines and growth factors such as CNTF during the regenerative phase after focal demyelination (Huang et al., 2011) may underlie the necessity of Stat3 signaling for OL differentiation and myelin repair. Interestingly, Stat3 transcript is also moderately but significantly increased in the lesion area during the regenerative phase after focal demyelination (Huang et al., 2011).

Stat3 is ubiquitously expressed and is responsible for orchestrating many cellular responses following its activation, which are likely to be cell lineage and context specific. As such Stat3 activation is likely to have a multifaceted role during demyelinating and myelin repair events. For instance, Stat3 activation is required for encephalitogenic Th17 cell development and autoimmune demyelination and appears to be dysregulated in MS (Benveniste et al., 2014). Increased level of phosphorylated Stat3 has been detected in cortical neurons in MS brains (Dutta et al., 2007) and in subsets of astrocytes and some microglia/macrophages and MBP^+ OLs in the white matter adjacent to active lesions (Lu et al., 2013). *NF-L* driven ablation of *Stat3* in neurons did not affect developing motoneurons when they physiologically depend on neurotrophic factors for survival, but impaired their survival after axotomy in the adult mice (Schweizer et al., 2002). Moreover, no major brain defects were

identified when *Stat3* is conditionally deleted in neurons and glia using the *Nestin* promoter (Gao et al., 2004). Similarly, mice with astrocyte specific *Stat3* deletion exhibited normal CNS development (Herrmann et al., 2008; Monteiro de Castro et al., 2015), but had less astrocyte activation after LPC-induced focal demyelination of spinal cord white matter and subsequently diminished remyelination by oligodendrocytes (Monteiro de Castro et al., 2015), which also suggests that successful remyelination by oligodendrocytes requires factors produced by astrocytes in a Stat3-dependent manner in the injury model. As *Olig1* mediated Cre recombination selectively targets OL lineage cells, our current study reveals that Stat3 signaling in OL lineage cells, while dispensable for myelination during development, is critical for myelin repair processes after focal demyelinating injury. Inactivating Stat3 signaling in OL lineage cells did not prevent OL progenitor production or microglia/macrophage and astrocyte activation after injury, but significantly impaired the generation of mature OLs and remyelination in comparison with lesioned littermate controls. The extract mechanisms by which the oligodendroglial Stat3 signaling pathway promotes myelin repair after demyelinating injury in the adult brain remain to be determined. In particular, what extracellular signals activate Stat3 in OLs in the context of demyelinating injury, how Stat3 activation promotes OL differentiation, whether Stat3 activation is preferably required for the survival of newly formed mature OLs, and moreover, what downstream targets following oligodendroglial Stat3 activation are critical for the regenerative process are a few important aspects that require further investigation.

In summary, our current study demonstrates that Stat3 activation in oligodendrocytes has a protective and beneficial role as it facilitates myelin repair after demyelinating injury in the adult CNS. To date, accumulating evidence has pointed to an apparent distinct role of Stat3 activation between cells of the CNS and those of the periphery during neuroinflammatory events and raised the question that while Stat3 pathway inhibition in lymphocytes may be beneficial for inflammatory demyelinating diseases, the inhibition of this same pathway in glia may in fact impede CNS regenerative responses and prove detrimental. Our findings also suggest that defining theStat3-dependentmolecular pathway in oligodendrocytes after demyelinating insult may reveal novel therapeutic targets for myelin repair.

Supplementary Material

Refer to Web version on PubMed Central for supplementary material.

Acknowledgments

We would like to thank Dr. Shizuo Akira (Osaka University, Japan) for the generous gift of $Stat3^{flox}$ mice and Dr. John DiGiovanni (University of Texas Anderson Cancer Center) for shipping the mouse colony. We are grateful to Li lab members for technical assistance and discussion. This research was funded in part by NIH grant R01NS060017 (JL), the National Multiple Sclerosis Society research grant RG4586 (JL) and Postdoctoral Fellowship FG1937 (AJS).

Appendix A. Supplementary data

Supplementary data to this article can be found online at http://dx.doi.org/10.1016/j.nbd.2016.03.023.

References

Albrecht PJ, Enterline JC, Cromer J, Levison SW. CNTF-activated astrocytes release a soluble trophic activity for oligodendrocyte progenitors. Neurochem Res. 2007; 32(2):263–271. [PubMed: 17004130]

Barres BA, Schmid R, Sendnter M, Raff MC. Multiple extracellular signals are required for long-term oligodendrocyte survival. Development. 1993; 118(1):283–295. [PubMed: 8375338]

Barres BA, Burne JF, Holtmann B, Thoenen H, Sendtner M, Raff MC. Ciliary neurotrophic factor enhances the rate of oligodendrocyte generation. Mol Cell Neurosci. 1996; 8(2–3):146–156.

Benveniste EN, Liu Y, McFarland BC, Qin H. Involvement of the janus kinase/signal transducer and activator of transcription signaling pathway in multiple sclerosis and the animal model of experimental autoimmune encephalomyelitis. J Interf Cytokine Res. 2014; 34(8):577–588.

Blakemore WF. Observations on oligodendrocyte degeneration, the resolution of status spongiosus and remyelination in cuprizone intoxication in mice. J Neurocytol. 1972; 1(4):413–426. [PubMed: 8530973]

Blakemore WF. Remyelination of the superior cerebellar peduncle in the mouse following demyelination induced by feeding cuprizone. J Neurol Sci. 1973; 20(1):73–83. [PubMed: 4744512]

Bonni A, Sun Y, Nadal-Vicens M, Bhatt A, Frank DA, Rozovsky I, Stahl N, Yancopoulos GD, Greenberg ME. Regulation of gliogenesis in the central nervous system by the JAK-STAT signaling pathway. Science. 1997; 278(5337):477–483. [PubMed: 9334309]

Bromberg JF, Wrzeszczynska MH, Devgan G, Zhao Y, Pestell RG, Albanese C, Darnell JE Jr. Stat3 as an oncogene. Cell. 1999; 98(3):295–303. [PubMed: 10458605]

Butzkueven H, Zhang JG, Soilu-Hanninen M, Hochrein H, Chionh F, Shipham KA, Emery B, Turnley AM, Petratos S, Ernst M, et al. LIF receptor signaling limits immune-mediated demyelination by enhancing oligodendrocyte survival. Nat Med. 2002; 8(6):613–619. [PubMed: 12042813]

Chen Y, Balasubramaniyan V, Peng J, Hurlock EC, Tallquist M, Li J, Lu QR. Isolation and culture of rat and mouse oligodendrocyte precursor cells. Nat Protoc. 2007; 2(5):1044–1051. [PubMed: 17546009]

Compston A, Coles A. Multiple sclerosis. Lancet. 2008; 372(9648):1502–1517. [PubMed: 18970977]

Dell'Albani P, Kahn MA, Cole R, Condorelli DF, Giuffrida-Stella AM, de Vellis J. Oligodendroglial survival factors, PDGF-AA and CNTF, activate similar JAK/STAT signaling pathways. J Neurosci Res. 1998; 54(2):191–205. [PubMed: 9788278]

Deverman BE, Patterson PH. Exogenous leukemia inhibitory factor stimulates oligodendrocyte progenitor cell proliferation and enhances hippocampal remyelination. J Neurosci. 2012; 32(6): 2100–2109. [PubMed: 22323722]

Doerflinger NH, Macklin WB, Popko B. Inducible site-specific recombination in myelinating cells. Genesis. 2003; 35(1):63–72. [PubMed: 12481300]

Dutta R, McDonough J, Chang A, Swamy L, Siu A, Kidd GJ, Rudick R, Mirnics K, Trapp BD. Activation of the ciliary neurotrophic factor (CNTF) signalling pathway in cortical neurons of multiple sclerosis patients. Brain. 2007; 130(Pt 10):2566–2576. [PubMed: 17898009]

Dziennis S, Alkayed NJ. Role of signal transducer and activator of transcription 3 in neuronal survival and regeneration. Rev Neurosci. 2008; 19(4–5):341–361. [PubMed: 19145989]

Emery B, Cate HS, Marriott M, Merson T, Binder MD, Snell C, Soo PY, Murray S, Croker B, Zhang JG, et al. Suppressor of cytokine signaling 3 limits protection of leukemia inhibitory factor receptor signaling against central demyelination. Proc Natl Acad Sci U S A. 2006; 103(20):7859–7864. [PubMed: 16682639]

Etxeberria A, Mangin J-M, Aguirre A, Gallo V. Adult-born SVZ progenitors receive transient synapses during remyelination in corpus callosum. Nat Neurosci. 2010; 13(3):287–289. [PubMed: 20173746]

Franklin RJM. Why does remyelination fail in multiple sclerosis? Nat Rev Neurosci. 2002; 3(9):705–714. [PubMed: 12209119]

Franklin RJM, ffrench-Constant C. Remyelination in the CNS: from biology to therapy. Nat Rev Neurosci. 2008; 9(11):839–855. [PubMed: 18931697]

Franklin, BJ.; Paxinos, G. The Mouse Brain in Stereotaxic Coordinates. Academic Press; New York: 2008. p. 162

Franklin RJM, ffrench-Constant C, Edgar JM, Smith KJ. Neuroprotection and repair in multiple sclerosis. Nat Rev Neurol. 2012; 8(11):624–634. [PubMed: 23026979]

Gao Q, Wolfgang MJ, Neschen S, Morino K, Horvath TL, Shulman GI, Fu XY. Disruption of neural signal transducer and activator of transcription 3 causes obesity, diabetes, infertility, and thermal dysregulation. Proc Natl Acad Sci U S A. 2004; 101(13):4661–4666. [PubMed: 15070774]

He F, Ge W, Martinowich K, Becker-Catania S, Coskun V, Zhu W, Wu H, Castro D, Guillemot F, Fan G, et al. A positive autoregulatory loop of Jak-STAT signaling controls the onset of astrogliogenesis. Nat Neurosci. 2005; 8(5):616–625. [PubMed: 15852015]

Herrmann JE, Imura T, Song B, Qi J, Ao Y, Nguyen TK, Korsak RA, Takeda K, Akira S, Sofroniew MV. STAT3 is a critical regulator of astrogliosis and scar formation after spinal cord injury. J Neurosci. 2008; 28(28):7231–7243. [PubMed: 18614693]

Huang JK, Jarjour AA, Oumesmar BN, Kerninon C, Williams A, Krezel W, Kagechika H, Bauer J, Zhao C, Baron-Van Evercooren A, et al. Retinoid X receptor gamma signaling accelerates CNS remyelination. Nat Neurosci. 2011; 14:45–53. [PubMed: 21131950]

Irvine KA, Blakemore WF. Remyelination protects axons from demyelination-associated axon degeneration. Brain. 2008; 131(6):1464–1477. [PubMed: 18490361]

Ishibashi T, Dakin KA, Stevens B, Lee PR, Kozlov SV, Stewart CL, Fields RD. Astrocytes promote myelination in response to electrical impulses. Neuron. 2006; 49(6):823–832. [PubMed: 16543131]

Ishibashi T, Lee PR, Baba H, Fields RD. Leukemia inhibitory factor regulates the timing of oligodendrocyte development and myelination in the postnatal optic nerve. J Neurosci Res. 2009; 87(15):3343–3355. [PubMed: 19598242]

Kerr BJ, Patterson PH. Leukemia inhibitory factor promotes oligodendrocyte survival after spinal cord injury. Glia. 2005; 51(1):73–79. [PubMed: 15779090]

Kim S, Steelman AJ, Koito H, Li J. Astrocytes promote TNF-mediated toxicity to oligodendrocyte precursors. J Neurochem. 2011; 116(1):53–66. [PubMed: 21044081]

Kim S, Steelman AJ, Zhang Y, Kinney HC, Li J. Aberrant upregulation of astroglial ceramide potentiates oligodendrocyte injury. Brain Pathol. 2012; 22:41–57. [PubMed: 21615590]

Laterza C, Merlini A, De Feo D, Ruffini F, Menon R, Onorati M, Fredrickx E, Muzio L, Lombardo A, Comi G, et al. iPSC-derived neural precursors exert a neuroprotective role in immune-mediated demyelination via the secretion of LIF. Nat Commun. 2013; 4:2597. [PubMed: 24169527]

Li J, Ramenaden ER, Peng J, Koito H, Volpe JJ, Rosenberg PA. Tumor necrosis factor {alpha} mediates lipopolysaccharide-induced microglial toxicity to developing oligodendrocytes when astrocytes are present. J Neurosci. 2008; 28(20):5321–5330. [PubMed: 18480288]

Linker RA, Maurer M, Gaupp S, Martini R, Holtmann B, Giess R, Rieckmann P, Lassmann H, Toyka KV, Sendtner M, et al. CNTF is a major protective factor in demyelinating CNS disease: a neurotrophic cytokine as modulator in neuroinflammation. Nat Med. 2002; 8(6):620–624. [PubMed: 12042814]

Louis JC, Magal E, Takayama S, Varon S. CNTF protection of oligodendrocytes against natural and tumor necrosis factor-induced death. Science (New York, NY). 1993; 259(5095):689–692.

Lu QR, Sun T, Zhu Z, Ma N, Garcia M, Stiles CD, Rowitch DH. Common developmental requirement for Olig function indicates a motor neuron/oligodendrocyte connection. Cell. 2002; 109(1):75–86. [PubMed: 11955448]

Lu Z, Hu X, Zhu C, Wang D, Zheng X, Liu Q. Overexpression of CNTF in mesenchymal stem cells reduces demyelination and induces clinical recovery in experimental autoimmune encephalomyelitis mice. J Neuroimmunol. 2009; 206(1–2):58–69. [PubMed: 19081144]

Lu JQ, Power C, Blevins G, Giuliani F, Yong VW. The regulation of reactive changes around multiple sclerosis lesions by phosphorylated signal transducer and activator of transcription. J Neuropathol Exp Neurol. 2013; 72(12):1135–1144. [PubMed: 24226263]

Marriott MP, Emery B, Cate HS, Binder MD, Kemper D, Wu Q, Kolbe S, Gordon IR, Wang H, Egan G, et al. Leukemia inhibitory factor signaling modulates both central nervous system demyelination and myelin repair. Glia. 2008; 56(6):686–698. [PubMed: 18293407]

Modi KK, Sendtner M, Pahan K. Up-regulation of ciliary neurotrophic factor in astrocytes by aspirin: implications for remyelination in multiple sclerosis. J Biol Chem. 2013; 288(25):18533–18545. [PubMed: 23653362]

Monteiro de Castro G, Deja NA, Ma D, Zhao C, Franklin RJM. Astrocyte activation via Stat3 signaling determines the balance of oligodendrocyte versus Schwann cell remyelination. Am J Pathol. 2015; 185(9):2431–2440. [PubMed: 26193667]

Nave KA. Myelination and support of axonal integrity by glia. Nature. 2010; 468(7321):244–252. [PubMed: 21068833]

Schneider CA, Rasband WS, Eliceiri KW. NIH Image to ImageJ: 25 years of image analysis. Nat Methods. 2012; 9(7):671–675. [PubMed: 22930834]

Schweizer U, Gunnersen J, Karch C, Wiese S, Holtmann B, Takeda K, Akira S, Sendtner M. Conditional gene ablation of Stat3 reveals differential signaling requirements for survival of motoneurons during development and after nerve injury in the adult. J Cell Biol. 2002; 156(2): 287–298. [PubMed: 11807093]

Stankoff B, Aigrot MS, Noel F, Wattilliaux A, Zalc B, Lubetzki C. Ciliary neurotrophic factor (CNTF) enhances myelin formation: a novel role for CNTF and CNTF-related molecules. J Neurosci. 2002; 22(21):9221–9227. [PubMed: 12417647]

Steelman AJ, Thompson JP, Li J. Demyelination and remyelination in anatomically distinct regions of the corpus callosum following cuprizone intoxication. Neurosci Res. 2012; 72(1):32–42. [PubMed: 22015947]

Steelman AJ, Smith R 3rd, Welsh CJ, Li J. Galectin-9 protein is up-regulated in astrocytes by tumor necrosis factor and promotes encephalitogenic T-cell apoptosis. J Biol Chem. 2013; 288(33): 23776–23787. [PubMed: 23836896]

Takeda K, Kaisho T, Yoshida N, Takeda J, Kishimoto T, Akira S. Stat3 activation is responsible for IL-6-dependent T cell proliferation through preventing apoptosis: generation and characterization of T cell-specific Stat3-deficient mice. J Immunol. 1998; 161(9):4652–4660. [PubMed: 9794394]

Vernerey J, Macchi M, Magalon K, Cayre M, Durbec P. Ciliary neurotrophic factor controls progenitor migration during remyelination in the adult rodent brain. J Neurosci. 2013; 33(7):3240–3250. [PubMed: 23407977]

Wegener A, Deboux C, Bachelin C, Frah M, Kerninon C, Seilhean D, Weider M, Wegner M, Nait-Oumesmar B. Gain of Olig2 Function in Oligodendrocyte Progenitors Promotes Remyelination. 2015:120–135.

Williams DA, Tao W, Yang F, Kim C, Gu Y, Mansfield P, Levine JE, Petryniak B, Derrow CW, Harris C, et al. Dominant negative mutation of the hematopoietic-specific Rho GTPase, Rac2, is associated with a human phagocyte immunodeficiency. Blood. 2000; 96(5):1646–1654. [PubMed: 10961859]

Xie TX, Wei D, Liu M, Gao AC, Ali-Osman F, Sawaya R, Huang S. Stat3 activation regulates the expression of matrix metalloproteinase-2 and tumor invasion and metastasis. Oncogene. 2004; 23(20):3550–3560. [PubMed: 15116091]

Xin M, Yue T, Ma Z, Wu F-f, Gow A, Lu QR. Myelinogenesis and axonal recognition by oligodendrocytes in brain are uncoupled in Olig1-null mice. J Neurosci. 2005; 25(6):1354–1365. [PubMed: 15703389]

Zhang Y, Taveggia C, Melendez-Vasquez C, Einheber S, Raine CS, Salzer JL, Brosnan CF, John GR. Interleukin-11 potentiates oligodendrocyte survival and maturation, and myelin formation. J Neurosci. 2006; 26(47):12174–12185. [PubMed: 17122042]

Zhang J, Zhang Y, Dutta DJ, Argaw AT, Bonnamain V, Seto J, Braun DA, Zameer A, Hayot F, Lopez CB, et al. Proapoptotic and antiapoptotic actions of Stat1 versus Stat3 underlie neuroprotective and immunoregulatory functions of IL-11. J Immunol. 2011; 187(3):1129–1141. [PubMed: 21709156]

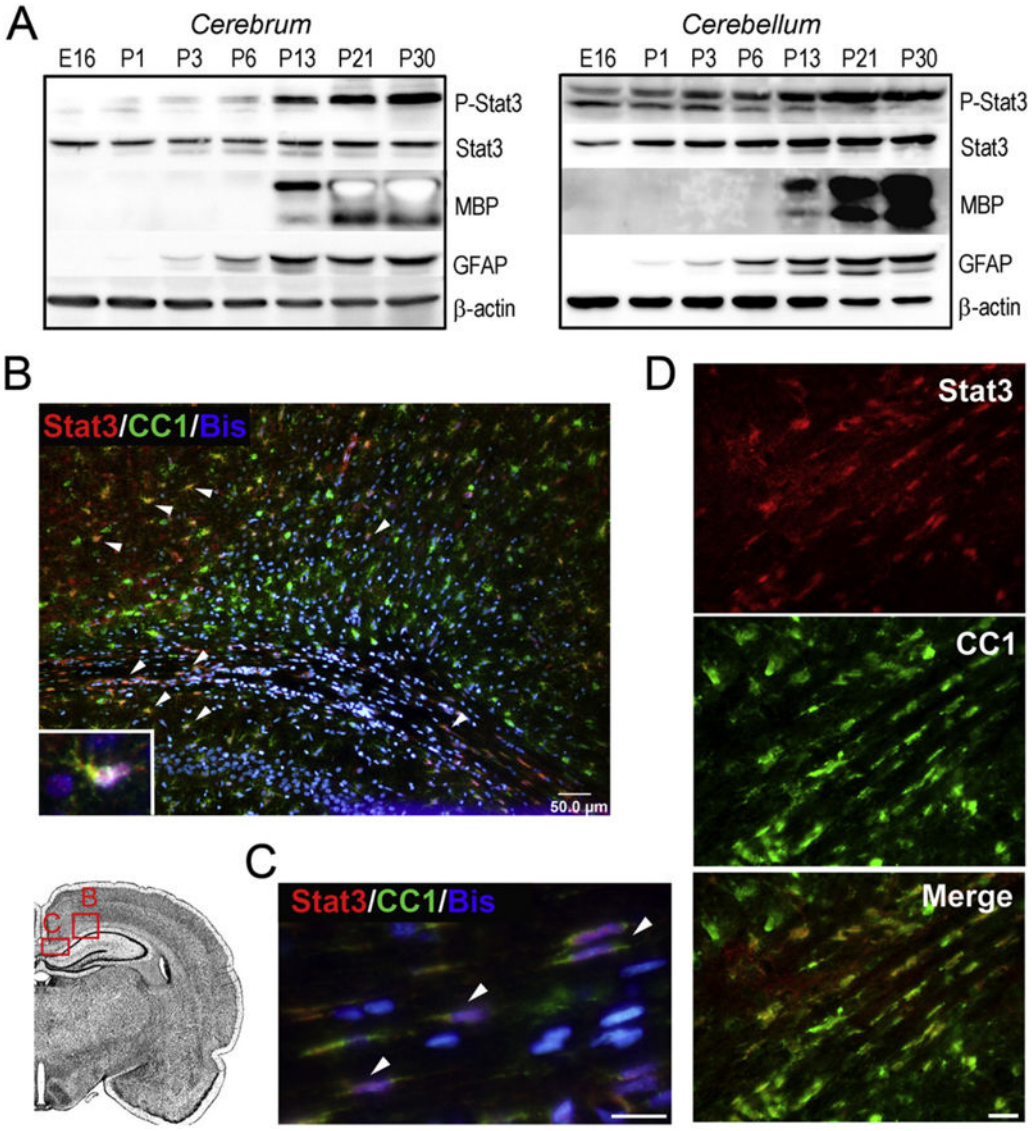

Fig. 1.

Expression of Stat3 in the developing rodent brain. Activation of Stat3 corresponds to the onset of CNS myelination. A, The level of phosphorylated Stat3 (Y705), Stat3, MBP, GFAP and β-actin was determined by Western blotting analyses of cerebrum and cerebellum at embryonic day 16 (E16) and postnatal (P) days 1, 3, 6, 13, 21 and 30. B–D, Representative micrographs of P14 rat brain sections immunostained for Stat3 (red), oligodendrocyte marker CC1 (green) and nuclei (blue) in the cingulate gyrus (B, boxed region in the sketch) and the corpus callosum (C, D). Colocalization of Stat3 signal to $CC1^+$ cells at higher magnification is illustrated in the insert of B and in C and D. Nuclei were visualized with Hoechst 33258 (bis-benzimide). Scale bars, 50 μm in B; 10 μm in C, D.

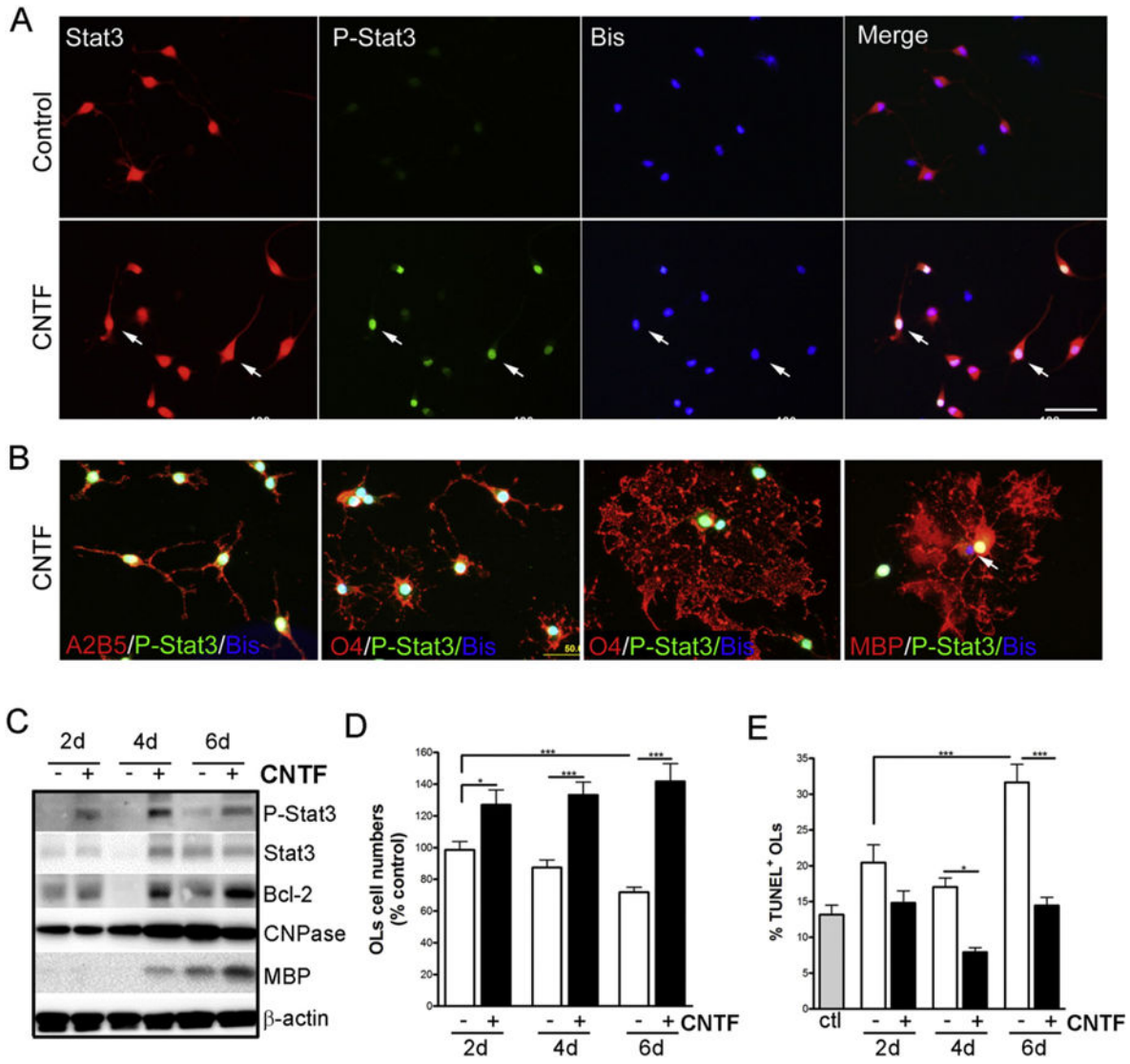

Fig. 2.

CNTF activates Stat3 and promotes OL lineage cell survival and differentiation in vitro. Primary rat OL lineage cells were treated with CNTF (10 ng/ml) for up to 6 days. A–B, CNTF treatment (30–60 min) induced Stat3 activation and nuclear translocation (A) independent of OL lineage cell development stages (B). Results are representative of 3 independent experiments. Scale bar, 100 μm. C, Western blot showing the effect of CNTF treatment on Stat3 activation, total Stat3, Bcl-2, CNPase, MBP and β-actin expression in OLs. Results are representative of 3 independent experiments. D–E, The effect of CNTF treatment on OL viability as determined by changes in cell number (D) with respect to controls and the percentage of TUNEL^{+} OLs (E). Results are means ± S.D. of 21 20× fields per condition analyzed in triplicate. *, $p \leq 0.05$; ***, $p \leq 0.001$.

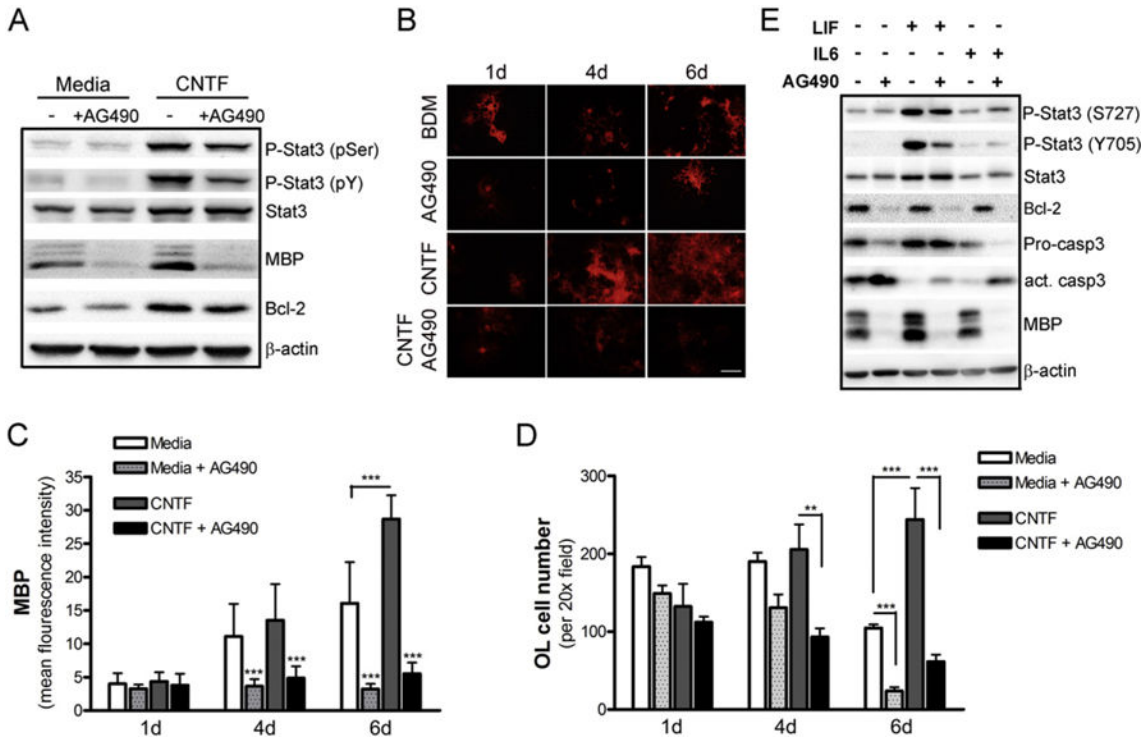

Fig. 3.

Pharmacological inhibition of JAK2 signaling decreases Stat3 activity and abrogates CNTF-mediated effects on oligodendrocytes. Rat OLs were pretreated with vehicle or AG490 (10 μM) for 1 h prior to stimulation with or without CNTF (10 ng/ml). A, The effect of CNTF and AG490 on Stat3 phosphorylation and MBP and Bcl-2 expression as determined by Western blot analysis. β-actin was used as a loading control. Data are representative of 3 experiments. B–D, AG490 prevented CNTF-induced OL maturation. OLs were stimulated as indicated for 1, 4 and 6 days, and mature OLs were determined by immunostaining for MBP and quantified by the mean fluorescence intensity (C) and total OL cell number determined by cell counting (D). Results are means ± S.D. of 14–16 20× fields per condition in triplicate. **, $p \leq 0.01$; ***, $p \leq 0.001$. Scale bar, 50 μm. E, OLs were pretreated with vehicle or AG490 for 1 h prior to stimulation with or without LIF (10 ng/ml) or IL-6 (10 ng/ml) for 4 days. Stat3 phosphorylation and MBP, Bcl-2, pro-caspase3 (Pro-casp3) and cleaved/active caspase3 (act. casp3) expression was determined by Western blot analysis.

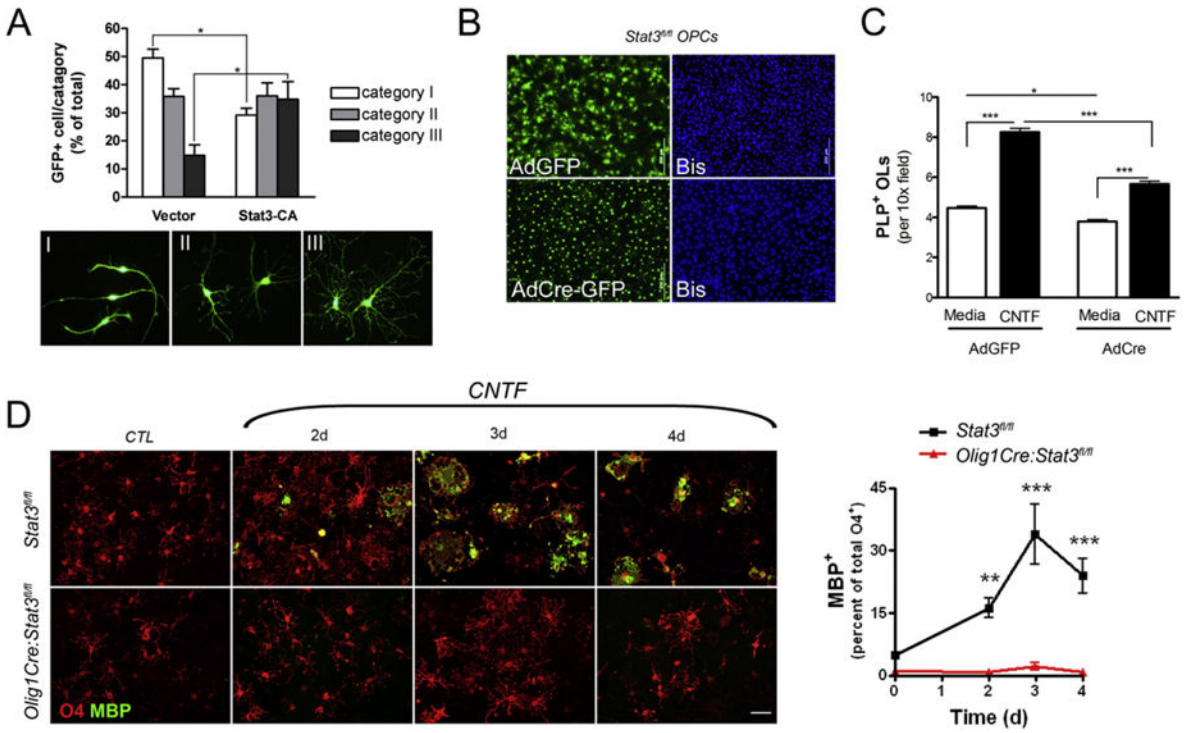

Fig. 4.

Stat3 is required to transduce CNTF-mediated effects on oligodendrocytes. A, Rat OPCs were transfected with retroviral vector containing GFP or constitutively active Stat3 and GFP for 3 days. The percentage of OPCs displaying primary (I), secondary (II) and tertiary (III) branching was determined. Results are means ± s.e.m. of 223–256 cells analyzed from 6 separate coverslips and are representative of 3 independent experiments. B–C, Mouse mixed glial cultures were derived from *Stat3*$^{fl/fl}$ mice were transfected with adenovirus containing GFP (AdGFP) or Cre recombinase and GFP (AdCre-GFP). Following transfection and 1 day of recovery the cultures were treated with or without CNTF (10 ng/ml) for 3 days. B, Representative micrographs showing efficiency of adenoviral transfection. Scale bar, 20 μm. C, The effect of AdCre mediated Stat3 deletion on CNTF-induced OL maturation as determined by counting PLP$^+$ OLs. Results are means ± s.e.m. of over 200 fields per condition. D, Representative micrographs of mouse mixed glia derived from *Stat3*$^{fl/fl}$ or *Olig1Cre:Stat3*$^{fl/fl}$ mice treated with CNTF (10 ng/ml) for 2, 3 and 4 days (left). The percent of mature MBP$^+$ (green) vs. total O4$^+$ (red) cells in each culture was determined by immunocytochemistry (left). Quantitative results are means ± s.e.m. of 6 10× fields per genotype per time-point and are representative of 3 independent experiments.

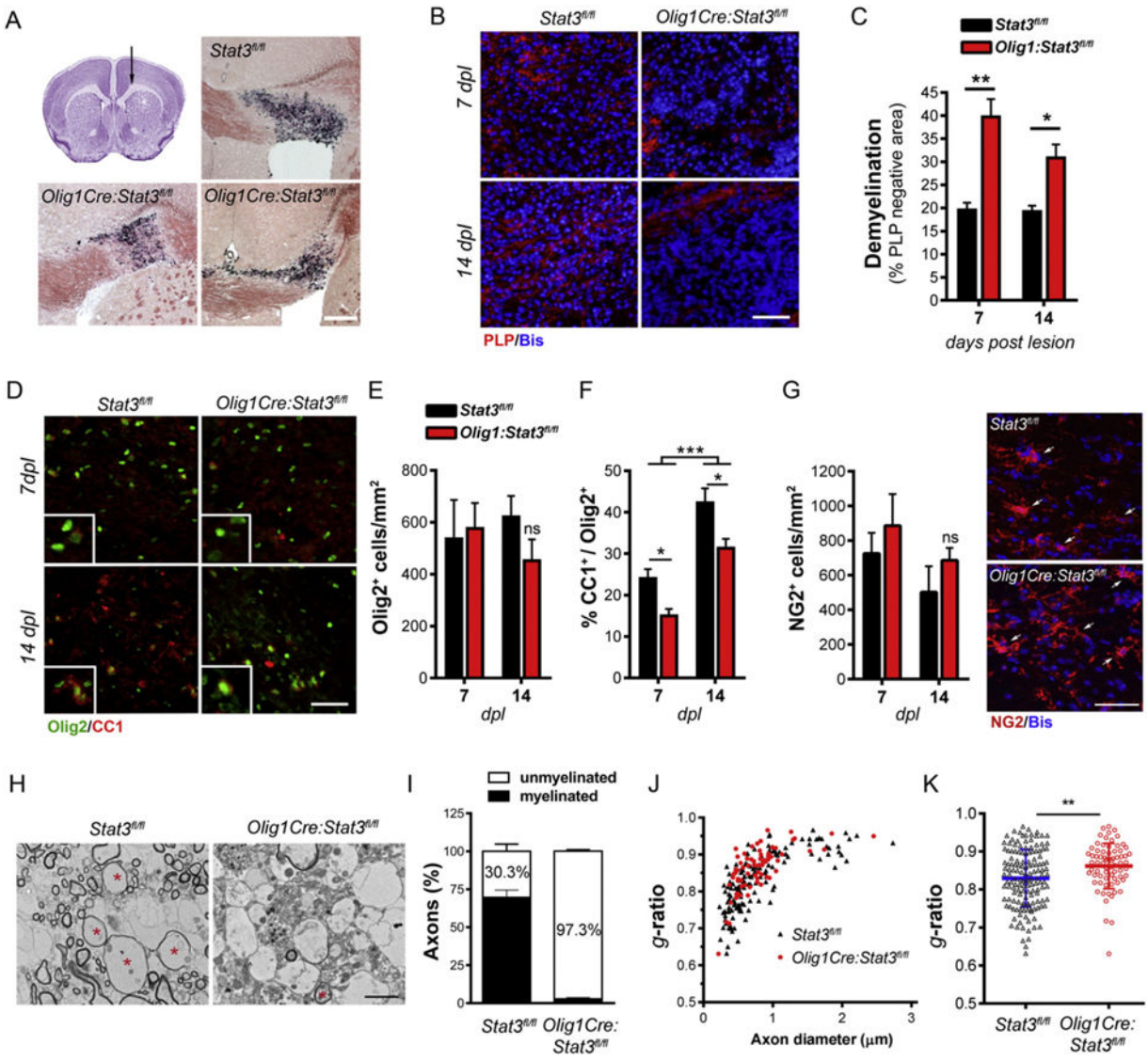

Fig. 5.

Conditional deletion of *Stat3* in oligodendrocyte lineage cells impedes remyelination.A,Scheme of LPC-induced focal demyelination. Focal demyelination was induced in *Stat3*$^{fl/fl}$ and *Olig1Cre:Stat3*$^{fl/fl}$ mice through stereotaxic injection of LPC into the rostral corpus callosum region (top left) and the extent of myelin repair was examined at 7 and 14 days post lesion (dpl). Myelin was visualized with Oil red O (ORO) staining of coronal sections of LPC-injected mice. Representative ORO images of control and mutant mice at 7 dpl were shown. Myelin debris as indicated by black/purple ORO signal is prominent in 7 dpl tissues. Scale bar, 250 μm. B–C, Demyelination was significantly higher in *Olig1Cre:Stat3*$^{fl/fl}$ mice as compared to littermate control *Stat3*$^{fl/fl}$ mice as quantified by analyzing the percent of PLP-negative area over the lesion area. D–F, Representative double immunostaining images and quantification of the number of Olig2^{+} OL lineage cells and the proportion of mature CC1^{+} OLs in the lesion areas of control and mutant mice at 7 dpl and 14 dpl. G, The number of NG2^{+} progenitor cells in the lesion is comparable between the two

genotypes at both 7 dpl and 14 dpl. Representative images of NG2 immunostaining at 14 dpl. Results (B–G) represent the means ± s.e.m. of 3–5 mice per group and 3–6 sections per mouse were counted. *, $p \leq 0.05$; **, $p \leq 0.01$; ***, $p < 0.001$. Scale bars, 50 μm. H, Ultrastructural microscopy shows many remyelinated axons (asterisks) in control mice compared to axons that remained demyelinated in the *Olig1Cre:Stat3*$^{fl/fl}$ mice at 14 dpl. Scale bar, 1 μm. I, Relative proportion of myelinated and unmyelinated axons in the lesion area of *Olig1Cre:Stat3*$^{fl/fl}$ mice compared to *Stat3*$^{fl/fl}$ mice at 14 dpl, showing that the majority of axons in the lesion area of the mutant mice remained demyelinated. Data are mean ± s.e.m. of images taken from 8–11 microscopic fields (2200×–7100×) per mouse and represent 2 mice per genotype. A total of 3308 axons for *Olig1Cre:Stat3*$^{fl/fl}$ mice and 1052 for *Stat3*$^{fl/fl}$ was analyzed. J–K, Scatter plots of *g*-ratio (axon diameter/fibre diameter) of individual myelinated axons in the lesion area at 14 dpl. The plots display *g*-ratios of individual axons and do not include unmyelinated axons (*g*-ratio = 1). The higher *g*-ratio in the mutant mice corresponds to impaired remyelination. **, $p < 0.001$. All *g*-ratios were analyzed from 7100× TEM images.

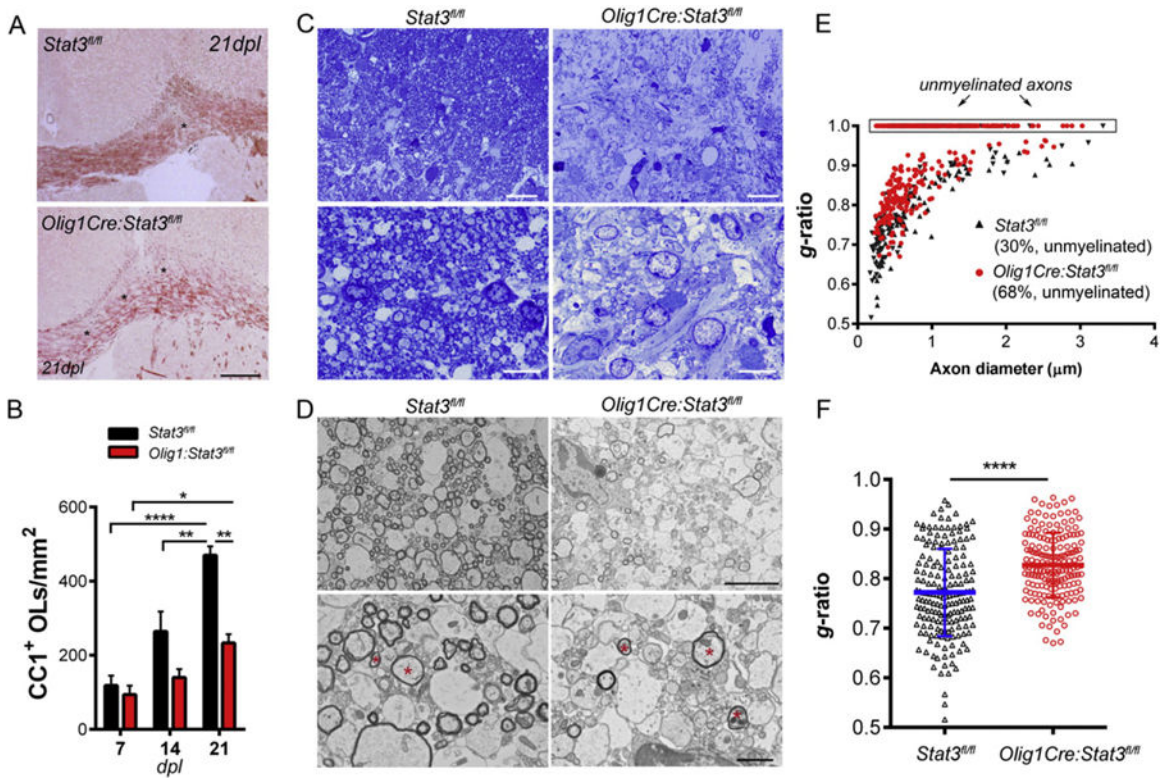

Fig. 6.

Persistent remyelination deficits in oligodendrocyte lineage-specific *Stat3* mutant mice after focal LPC injury. Impaired remyelination in *Olig1Cre:Stat3*$^{fl/fl}$ mice compared to littermate controls at 21 days post lesion. A, ORO staining of the corpus callosum of lesioned mice 3 weeks after LPC injection. Scale bars, 250 μm. B, Quantification of the density of mature CC1^{+} OLs in the lesion area at 7–21 dpl. Results represent the means ± s.e.m. of 3–5 mice per group. *, $p \leq 0.05$; **, $p \leq 0.01$; ****, $p < 0.0001$; One-way ANOVA. Scale bars, 50 μm. C, Light microscopy of methylene blue/azure II stained semi-thin sections of lesioned regions of *Olig1Cre:Stat3*$^{fl/fl}$ and *Stat3*$^{fl/fl}$ mice at 21 dpl. Data represent 2 mice per genotype. Scale bars, 20 μm (top); 10 μm (bottom). D, ultrastructural microscopy shows many remyelinated axons in *Stat3*$^{fl/fl}$ mice whereas many axons remained demyelinated in the mutant mice. Asterisks, examples of remyelinated axons. E–F, Quantifications of *g*-ratios of individual axons showing significantly less remyelination and thinner myelin sheaths, corresponding to higher *g*-ratios of remyelinated callosal axons in Stat3 mutant mice with respect to control *Stat3*$^{fl/fl}$ mice. ****, $p < 0.0001$.